V-Band and W-Band Broadband, Monolithic Distributed Frequency Multipliers

Eric Carman, Michael Case, Masayuki Kamegawa*, Ruai Yu, Kirk Giboney, and Mark Rodwell

Department of Electrical and Computer Engineering
University of California, Santa Barbara, CA 93106, (805) 893-3244
*Shimadzu Corporation, Kyoto, Japan

Abstract

Broadband V-Band and W-Band frequency multiplication is reported using soliton propagation on GaAs monolithic nonlinear transmission lines. With 24 dBm input a doubler attained 17.4 dBm peak output power with at least 52-63.1 GHz 3-dB bandwidth, and a tripler attained 12.8 dBm peak output power with at least 81-108.8 GHz 3-dB bandwidth. These multipliers, fabricated with 3-μm design rules on Gas and driven with lower frequency amplifiers, have applications as cost-effective signal sources in mm-wave communication and measurement systems.

Introduction

Schottky diode frequency multipliers driven by phase locked microwave generators are widely used as low phase noise millimeter-wave signal sources for receivers and instrumentation. Common multiplier implementations, however, are limited in either conversion efficiency or bandwidth. Implementations using Schottky diodes as nonlinear conductances cannot attain high conversion efficiencies, while implementations using lumped-element Schottky varactor diodes have reactive input and output impedances which cannot be matched efficiently over a broad bandwidth. As shown by Scott [1] and others [2]-[5] harmonic generation can also be performed on nonlinear transmission lines (NLTL's) [6], structures having periodically distributed nonlinear capacitance. Through soliton propagation on NLTL's, harmonic generation with broad bandwidth and high efficiency is possible.

In this work we have improved our previous results [5] by reducing skin losses and by introducing devices for V-Band and W-band output. Here, we report broadband harmonic generation in the 60 GHz band with 17.4 dBm output power, and harmonic generation in the 90 GHz band with 12.8 dBm output power. These devices do not compete directly with current HEMT power performance [7, 8], but since they are driven with lower frequency amplifiers and are processed with 3-μm design rules on GaAs, they are cost-effective sources of high frequency power.

Solitons on NLTLs

Solitons are pulse-like waveforms which propagate without distortion in media having both nonlinearity and dispersion. An NLTL, a ladder network of high-impedance transmission line sections periodically loaded with reverse-biased diodes (Fig. 1), exhibits nonlinearity from the diodes' voltage-variable capacitance and dispersion from the periodic network. NLTLs therefore support soliton propagation. If the diodes have capacitance $C_d(V)$, the interconnecting high-impedance line sections have characteristic impedance Z_L and electrical delay τ and if $C_d(V) > \tau/Z_L$, then the structure can be approximately modelled as an LC ladder network having $L = Z_L\tau$ and $C(V) = C_d(V) + \tau/Z_L$. In the small-signal limit at bias voltage V_{bias}, the line periodicity prevents propagation above the Bragg frequency, $f_b = 1/(\pi\sqrt{LC(V_{bias})})$.

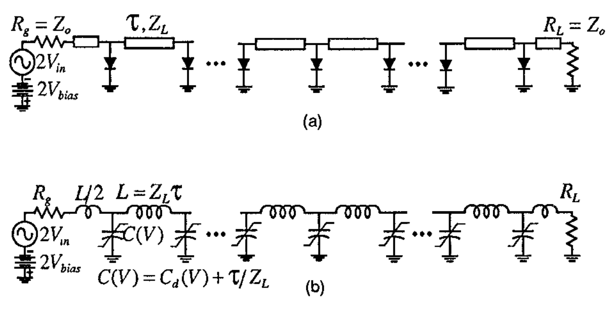

Figure 1: (a) Nonlinear transmission line circuit diagram, and its (b) L-C ladder network equivalent circuit.

Waveforms on NLTLs are described by a nonlinear differential-difference equation, one solution set of which is solitons, pulse waveforms which have propagation delay per NLTL section [9, 10]

$$T_d = \sqrt{LC_oV_o/V_{max}}\,\sinh^{-1}\left[\sqrt{\frac{V_{max}}{V_o}}\right], \quad (1)$$

and FWHM pulse width

$$T_{FWHM} = 1.212\sqrt{LC_oV_o/V_{max}} \quad (2)$$

where $C(V)$ is approximated as $C_o/(1 - V/V_o)$. On the NLTL, impulses of amplitude V_{max} having duration $T_{FWHM} > 1.212\sqrt{LC_oV_o/V_{max}}$ correspond to a nonlinear superposition of a set of solitons having differing amplitudes (i.e., different V_{max}'s) and hence differing per-section propagation delays T_d; if such an impulse is applied to the network, the input impulse will decompose into this set of two or more solitons during propagation. If instead of driving the NLTL with a single pulse, we drive it with a train of pulses (e.g.: a sine wave) then each pulse separates into a set of solitons, generating a waveform with multiple pulses per cycle and hence significant harmonic content. Harmonic generation is most efficient when the Bragg frequency eliminates spectral power above the desired harmonic.

Figure 2 shows measured output waveforms for an NLTL with f_b=35 GHz, 20 dBm input power, and -3.0 volt bias. The waveform in Figure 2(a) with 10 GHz input frequency and input pulse width, T_{FWHM} = 50 ps, shows three distinct solitons per cycle. The 40 GHz harmonic is above the 35 GHz Bragg frequency and so is suppressed. Figure 2(b), generated from a 14 GHz input frequency with input pulse width, T_{FWHM} = 35.7 ps, shows a waveform with primarily second harmonic output, since the third harmonic is above f_b. In general conversion to second harmonic is most efficient if $f_b/3 < \omega_1 < f_b/2$. This is also the maximum usable bandwidth of the device as a frequency doubler since an output filter with greater bandwidth than $f_b/3 < \omega_1 < f_b/2$ would pass harmonics at ω_1 or $3\omega_1$ depending on where ω_1 is in that range.

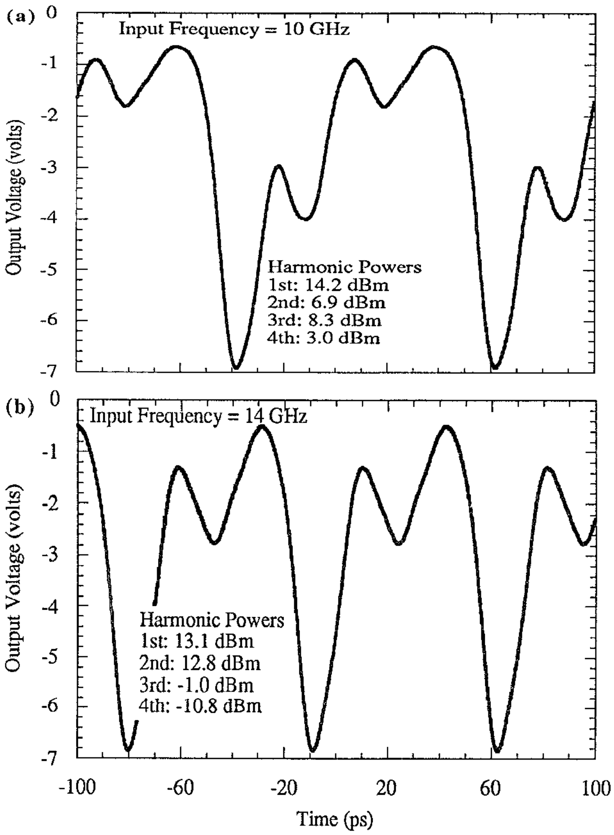

Figure 2: Experimentally observed waveforms exhibiting splitting of input sine wave into solitons for NLTL with f_b=35 GHz and -3.0 V bias. A 10 GHz input signal with T_{FWHM}=50 ps splits into three solitons while a 14 GHz input signal with T_{FWHM}=35.7 ps splits into two solitons.

Coupled Harmonics Model

Described instead in terms of coupled propagation of Fourier components, harmonics of ω_1 are generated by voltage-variable capacitance. Assume that

$$C(V) \cong C_o + C_1(V - V_{bias}) \tag{3}$$

and that the voltage V_n at the n^{th} diode has Fourier components at the fundamental ω_1 and the second harmonic $\omega_2 = 2\omega_1$,

$$V_n(t) = V_{bias} + V_{n1}\cos(\omega_1 t + \phi_1) + V_{n2}\cos(\omega_2 t + \phi_2). \tag{4}$$

The nonlinear capacitance term C_1 generates currents at ω_2 of

$$I_{d,n}^{\omega_1 \to \omega_2} = \left(C_1 \omega_1 V_{n1}^2/2\right)\sin(\omega_2 t + 2\phi_1), \tag{5}$$

at ω_1 of

$$I_{d,n}^{\omega_1, \omega_2 \to \omega_1} = \left(C_1 \omega_1 V_{n1} V_{n2}/2\right)\sin(\omega_1 t + \phi_2 - \phi_1), \tag{6}$$

and at higher harmonics of ω_1.

Neglecting harmonics above ω_2, which will not propagate if we choose $2\omega_1 < f_b < 3\omega_1$, these currents will cause the fundamental to exchange power with the second harmonic, which in the case of phase-matched fundamental and second harmonic [3,4], will generate a second harmonic wave whose amplitude grows with propagation distance. The second harmonic amplitude reaches a maximum after a distance of

$$n_{\max} \cong \pi/\omega_2 \left|T_P(\omega_2) - T_P(\omega_1)\right|. \tag{7}$$

With further propagation, the phase angle between the accumulated second harmonic wave amplitude and the second harmonic conversion current $I_{d,n}^{\omega_1 \to \omega_2}$ exceeds $\pi/2$, and the second harmonic amplitude decreases. To maximize conversion efficiency, the number of NLTL sections is selected to be approximately $n_{\max}$ in the center of the band from $f_b/3 < \omega_1 < f_b/2$.

Fabrication

The frequency multipliers are fabricated using a five mask process on GaAs molecular beam epitaxy material. Schottky diodes are formed on a semiinsulating GaAs substrate with an exponentially graded 425 nm thick N^- active layer whose doping variation with depth is $N^-(d) = N_o \exp(-d/d_o)$, where d is the distance from the wafer surface, N_o=2x10^{17}/cm^3 and d_o=225 nm. A buried 1 µm thick N^+ layer (6x10^{18}/cm^3 doping, 7 Ω per square sheet resistivity) provides the diode cathode connections. Ohmic contacts to the N^+ layer (with 0.02 Ω-mm resistivity) are formed by a 0.5 µm $NH_4OH/H_2O_2/H_2O$ recess etch, a self aligned AuGe-Ni-Au liftoff, and a rapid thermal anneal. Proton implantation using both 180 kev, 1.7x10^{15}/cm^2 and 100 kev, 4x10^{14}/cm^2, provides high isolation, defining diode contact areas and eliminating N^+ and N^- layer conductivities near the coplanar-waveguide sections, reducing dielectric losses. During implantation, a 1.7 µm Au - 1.0 µm polyimide mask protects ohmic contacts and diode active regions. The transmission lines are formed with a 200 Å Ti - 200 Å Pt - 2.4 µm Au liftoff; Schottky contacts result where the Ti-Pt-Au liftoff intersects the unimplanted N^- layer. At 3-µm design rules, the diodes have approximately 800 GHz zero-bias cutoff frequency where $f_{d,0} = 1/(2\pi C_d(0) r_d)$. By electroplating Au, airbridges are formed between the coplanar waveguide ground planes to eliminate unbalanced, coplanar strip type modes. Figure 3 shows a photograph of an NLTL section containing two diodes and an airbridge. Unlike our previous devices [5] where 90 Ω inductive line sections were used, the current devices use 75 Ω line sections. These have wider signal conductors and hence substantially lower skin loss.

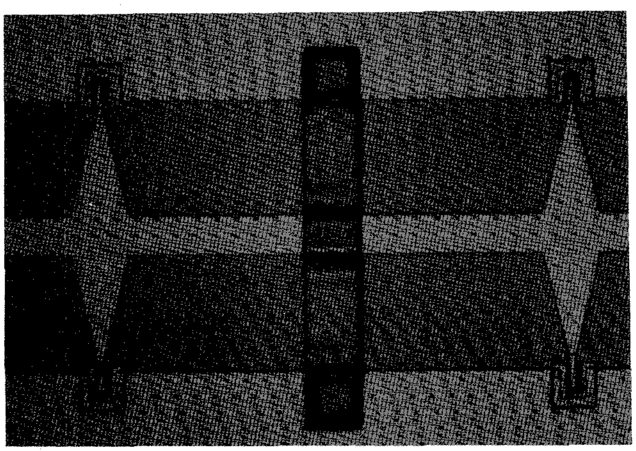

Figure 3: Photograph of NLTL line section including two diodes and an airbridge. The airbridge (center) is used to reduce unbalanced modes on the coplanar waveguide structure.

Results

In addition to the 9-18 GHz input doubler in Figure 2, we measured a doubler (f_b=69 GHz) and a tripler (f_b=99 GHz), both having a 26-40 GHz input band. The multiplier output waveforms were measured using integrated on-wafer 275 GHz bandwidth sampling circuits [11], and power spectra were obtained by numerical Fourier transformation. For the doubler, τ=3.1 ps and $C_d(V) \equiv C_{jo}/(1-V/\phi)^M$, where C_{jo}=105 fF, ϕ=1 volt and M=0.708. The tripler had τ=2.1ps, and C_{jo}=73.0 fF.

With 20 dBm input power at -3.0 V bias the K-Band doubler gives 12.8 dBm peak output power at 29 GHz and a 24.3-32.3 GHz 3-dB bandwidth. In Figures 3 and 4 experimental results are compared with harmonic-balance circuit simulations [12] for the V-Band and W-Band devices, measured with 24 dBm input power (10.0 V p-p). The V-Band doubler, biased at -4.6 volts, gives 17.4 dBm peak output power at 56 GHz and at least a 52-63.1 GHz 3-dB bandwidth (Figure 4). We were unable to make measurements below 52 GHz because of limitations in the source frequency range. The W-Band tripler, biased at -3.0 volts, attains better than 12 dBm output power from 81-103.5 GHz (Figure 5). The 3-dB bandwidth of the device is at least 81-108.8 GHz with source limitations below 81 GHz output frequency. For both high frequency devices, measurements agree with simulations to within approximately 2-dB, although the doubler simulation is shifted in frequency from the measured curve. Simulations indicate that diode reverse breakdown causes significant loss.

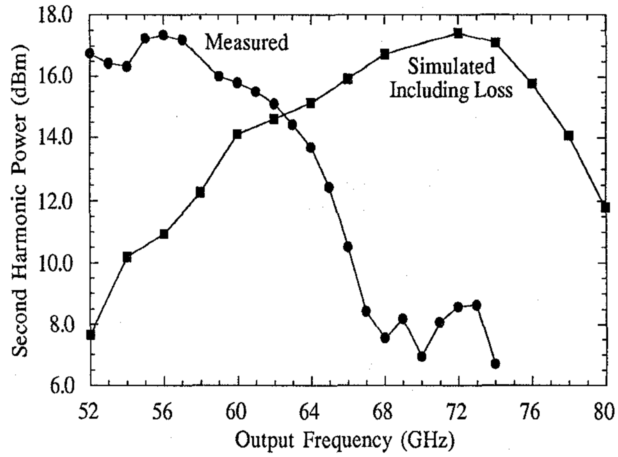

Figure 4: Measured and simulated curves of output power versus output frequency for frequency doubler with f_b=69 GHz and 24 dBm input power. The doubler is 5.4 mm long.

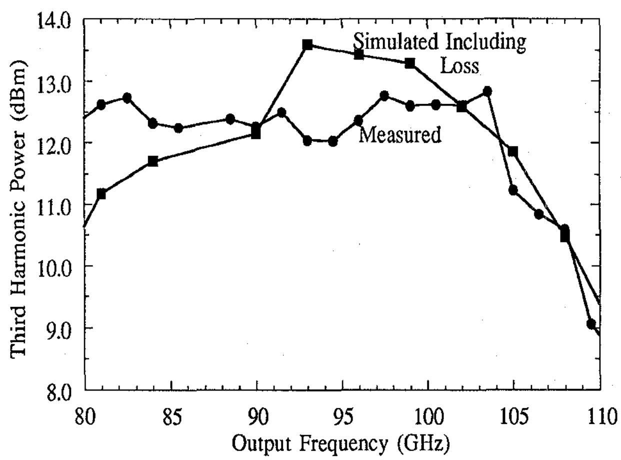

Figure 5: Measured and simulated curves of output power versus output frequency for tripler with f_b=99 GHz and 24 dBm input power. The tripler is 5.0 mm long.

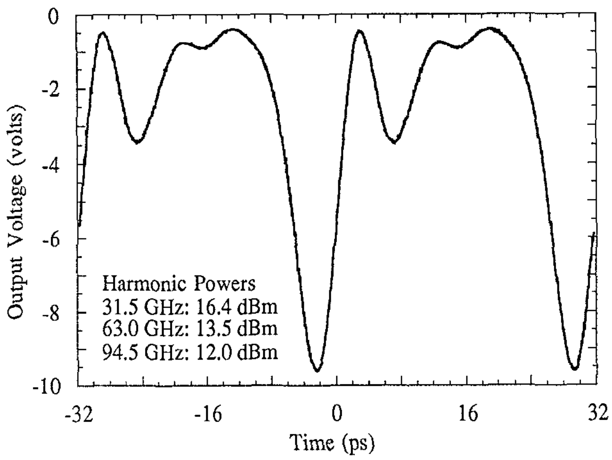

Figure 6: Measured output waveform for tripler with f_b=99 GHz at 31.5 GHz and 24 dBm input.

Summary

We have demonstrated broadband millimeter-wave distributed frequency multiplication in the V-band and W-band. The devices were designed without modelling breakdown effects, in which case expected conversion loss was 4 dB for the V-Band doubler and 10 dB for the W-Band tripler. Significant improvements in efficiency should be obtained if the breakdown voltage is increased. With 3-μm design rules on GaAs and lower frequency sources, these monolithic frequency multipliers can be used as cost-effective broadband signal sources for receivers and instrumentation in the 60 and 90 GHz bands.

Acknowledgment

We acknowledge generous equipment donations from Hewlett-Packard, Tektronix, and additional assistance from the Hughes Aircraft Company. This work was supported by the Air Force Office of Scientific Research under grant number AFOSR-89-0394.

References

[1] A. Scott, *Active and Nonlinear Wave Propagation in Electronics*. New York: Wiley-Interscience, 1970.

[2] R.A. Marsland, M.S. Shakouri, and D.M. Bloom, "Millimeter-wave generation on a nonlinear transmission line," *Electron. Lett.*, vol. 26, no. 16, pp. 1235-1236 Aug. 2, 1990.

[3] D. Jäger and F.J. Tegude, "Nonlinear wave propagation along periodic-loaded transmission line," *Appl. Phys.*, vol. 15, pp. 393-397, 1978.

[4] K.S. Champlin and D.R. Singh, "Small-signal second-harmonic generation by a nonlinear transmission line," *IEEE Trans. Microwave Theory Tech.*, vol. MTT-34, no. 3, pp. 351-353, Mar. 1986.

[5] E. Carman, K. Giboney, M. Case, M. Kamegawa, R. Yu, K. Abe, M.J.W. Rodwell, and J. Franklin, "28-39 GHz Distributed Harmonic Generation on a Soliton Nonlinear Transmission Line," *IEEE Microwave and Guided Wave Letters,* vol. 1, no. 2, pp. 28-31, Feb. 1991.

[6] M.J.W. Rodwell, M. Kamegawa, R. Yu, M. Case, E. Carman, and K. Giboney, "GaAs Nonlinear Transmission Lines for Picosecond Pulse Generation and Millimeter-Wave Sampling," *IEEE Trans.Microwave Theory and Tech*, vol. 39, no. 7, July 1991, and references therein.

[7] D.C. Streit et al, "High-Gain W-Band Pseudomorphic InGaAs Power HEMT's," *IEEE Electron. Device Lett.*, vol. EDL-12, no. 4, pp. 149-150, 1991.

[8] P.M. Smith et al, "A High Power, High Efficiency Pseudomorphic HEMT," *IEEE MTT-S Dig*., 1991, pp.717-720

[9] R. Hirota and K. Suzuki, "Theoretical and experimental studies of lattice solitons in nonlinear lumped networks," *Proc. IEEE*, vol. 61, no. 10, pp. 1483-1491, Oct. 1973.

[10] A. Scott, F.Y.F. Chu, and D.W. McLaughlin, "The soliton: a new concept in applied science," Proc. IEEE, vol. 61, pp. 1443-1482, Oct. 1973.

[11] R.Y. Yu, M. Case, M. Kamegawa, M. Sundaram, M.J.W. Rodwell, and A. W. Gossard, "275 GHz 3-mask integrated GaAs sampling circuit," *Electron. Lett.*, vol. 26, no. 13, pp. 949-951, June 21, 1990.

[12] LIBRA and Microwave SPICE, EEsof, Inc., 5601 Lindero Canyon Road, Westlake Village, CA, 91362